Generation and conversion of optical vortices in long-period helical core optical fibers

Constantine N. Alexeyev* and Maxim A. Yavorsky
Taurida National V. I. Vernadsky University, Vernadsky Prospekt, 4, Simferopol, 95007, Crimea, Ukraine
(Received 25 August 2008; published 30 October 2008)

We theoretically study generation and conversion of optical vortices (OVs) in long-period helical core fibers (HCFs) produced by drawing from a perform with an eccentric core. Solving scalar waveguide equation in the helical coordinates we demonstrate that in such fibers topologically induced corrections to scalar propagation constants lead to convergence of spectral curves. At their intersection points a resonance coupling takes place between the fundamental and the vortex modes, as well as the coupling between OVs, whose topological charges differ by unity. This coupling leads to energy exchange between the coupled modes, which is manifested either in conversion of the input fundamental mode into an OV or transformation of an OV into the OV with higher by 1 (or lower, depending on core's helicity) value of the topological charge. This effect can be used for creation of all-fiber generators of singular beams from regular input beams. We also study effect of ellipticity of the core's form on transformation properties of HCFs and show that this leads to splitting of resonance fiber's parameters, at which conversion of left and right circularly polarized input regular beams into OVs occurs. We prove that in long-period HCFs one can neglect this effect due to reduction of polarization mode dispersion in twisted fibers.

DOI: 10.1103/PhysRevA.78.043828 PACS number(s): 42.25.Bs, 42.81.Qb, 42.81.Bm

I. INTRODUCTION

Quite counterintuitively, in optics—the science of light—a number of phenomena are closely connected just with its absence. One such optical phenomenon that has recently drawn the attention of both theoreticians and experimenters are the optical vortices (OVs)—three-dimensional threads of darkness where the amplitude of the light field equals zero [1–3]. Although vortex phenomena are wide spread in nature and, in principle, could have been traced back in earlier research in optics, it was not realized until the paper by Nye and Berry [4] that vortices in electromagnetic fields are strongly connected with phase discontinuities or singularities. It has been noted that for a scalar field Ψ near the lines of zero amplitude defined as $\mathrm{Im}\,\Psi=\mathrm{Re}\,\Psi=0$ the lines of constant phase feature the presence of phase dislocations. Near the dislocation centers the phase gradient lines, which the energy flows along, were found to form closed vortexlike structures. Circulation of energy flow around the phase singularity point gives rise to a localized orbital angular momentum (OAM) associated with the OV [5,6]. In general, pure OVs as the states with well-defined OAM are very promising information carriers, in which information can be encoded in the OAM state [7–10]. In addition, since the field intensity of an OV has a pronounced dip in the center, the OV can be used for particle trapping and manipulation [11]. Using OVs one can overcome the Rayleigh diffraction limit, which finds its application in space research [12] and in singular beam microscopy [13]. The concept of the phase singularity proves to be seminal also for x rays [14]. One should also mention significance of OVs for creation of vortex states in Bose-Einstein condensate (BECs), which can be used for information storage [15], as well as generation of plasmon polaritons by OVs [16]. It is remarkable that, although vortex phenomena have been first demonstrated for the systems described by nonlinear equations, electromagnetic vortices are generic to the field governed by linear Maxwell's equations. Despite the differences in the governing equations, they feature common properties, even in such complicated cases as the case of random fields [17]. Moreover, being a six-component vectorial field, the electromagnetic field can possess of other types of singularities not present in purely scalar fields. Examples are vectorial or polarization singularities, whose presence is connected with the Stokes parameters field [18,19]. In addition, the presence of singularities is reported for the Poynting vector's field [20].

The growing range of application of OVs calls for reliable methods of their generation. To date, several techniques of OV generation have won general recognition, such as the generation of vortex-bearing beams from Hermite-Gaussian (HG) beams by lens converters [21]; generation of OVs from Gaussian beams (GBs) by spiral phase plates [22], and creation of OVs by computer-generated holograms [23]. Recently, other methods of OVs creation have been suggested. One of them concerns generation of OVs through spatial light modulation by liquid crystal cells [24]. OVs also appear in the process of light diffraction on dielectric wedges [25]. One should also mention application of metamaterials for generation and control of OVs [26]. All the described techniques, however, give birth to a free-space propagating OV. Meanwhile, to transmit the OV over distance by an optical fiber one has to couple such a free-space OV to the fiber. Although this problem can be solved [27], it is sometimes preferable to use the methods of direct excitation of OVs in fibers eliminating the free-space stage.

Some of such methods incorporate basic principles, on which the generation of free-space OVs is grounded. For example, the method of generation of OVs from the input HG beams by stress-applied optical fibers [28] exploits the similarity between astigmatic anisotropic fibers and lens converters. The other scheme of OV generation with the use of a phase mask [29] clearly resembles the spiral phase plate

*alexeyev@ccssu.crimea.ua

method [22]. However, certain methods of OV creation in fibers have no direct analogies among the free-space methods. Examples are methods concerning the use of twisted birefringent fibers, in which due to a specific helical dependence of the refractive index the modes are represented by pure OVs [30]. In our opinion, such "fiber-based" methods of OV generation are somewhat more convenient for the purposes of optical communication by fiber lines since a vortex created in the fiber is more easily coupled to another fiber than a vortex initially created in a free space.

In this paper we study theoretically generation and conversion of OVs by weakly guiding helical core fiber (HCFs). Such a type of fiber has been under consideration since the paper of Poole *et al.* on a mode coupler based on a fiber wrapped in a coiled wire of a constant pitch [31]. As is known, periodical microbendings induce the so-called path-length optical gratings in fibers [32], in which the optical path is periodically changed due to geometrical variations produced by bending. A sinusoidal bending proves to induce in the fiber the coupling between LP_{01} and LP_{11} modes (linearly polarized fiber modes where the first index stands for the orbital number and the second one- for the radial number of the mode) if the grating pitch equals to the intermodal beat length. For a special kind of a helical path-length grating, which is produced by winding a wire over a fiber, at certain conditions a resonance coupling takes place, at which the fundamental mode gets coupled to the combination of LP_{11} modes known at present as the OV. First reported in Ref. [31], this effect has also been demonstrated for helical fiber gratings [33]. In general, chiral fibers represent a special class of one-dimensional photonic crystals with a wide area of practical application [34,35]. For pitch values comparable with the wavelength they feature the presence of the spectrum gap [30], which causes their unique properties concerning OV transmission [36]. In the present paper we will focus our attention on long-period HCFs, which possess the property of transforming the incident GB into an OV. In particular, we will study another type of HCF, which has recently evoked much amount of interest in researchers. Two novel types of such fibers are manufactured via drawing from a specially designed perform [35] and by writing the helical core in the fiber by a CO_2 laser [37]. As has been emphasized in our recent paper [36], the HCFs described in Ref. [35] are characterized by the refractive index distribution that essentially differs from the one present in the bending-created helical gratings. For the time being, no experiments on the vortex generation in these types of HCFs have been reported, which explains our interest in the study of such fibers.

The aim of the present paper is to study theoretically the possibility of OV generation from the fundamental modes in HCFs produced by drawing from a specially tailored perform. We demonstrate that at certain values of the helix pitch a resonance coupling between the fundamental and the vortex modes occurs in such fibers. This wavelength-dependent coupling leads to a periodic conversion of the fundamental mode into the OV, and vice versa, which can be used for generation of an OV from the input fundamental mode. We also study the influence of the core's ellipticity on the splitting of resonance wavelengths, at which conversions of right and left circularly polarized fundamental modes into OVs takes place. We show that the resonance splitting is strongly reduced due to the effect of polarization mode dispersion (PMD) reduction in twisted-core fibers.

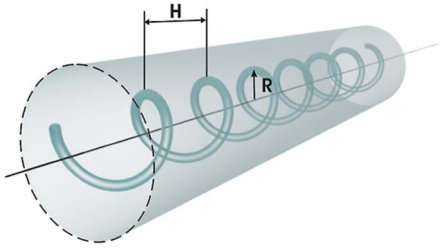

FIG. 1. (Color online) The model of a helical core fiber manufactured by drawing from a perform with an off-centered core.

II. WAVEGUIDE EQUATION IN THE HELICAL COORDINATES

Historically, helical path-length fiber gratings were first created by periodically bending the fiber in orthogonal planes [31]. This particular type of perturbation generates in the fiber the following distribution of the refractive index n [36]:

$$n(\rho,\vartheta,z) = \tilde{n}(\rho)\left[1 + \frac{\rho}{r_b}\cos(\vartheta - qz)\right], \tag{1}$$

where r_b is the radius of bending and (ρ,ϑ,z) are the cylindrical polar coordinates. Here and throughout a tilde denotes an axially symmetric function. This method of creation of helical gratings, in spite of its relative simplicity, has the main drawback concerned with the difficulty of maintaining the regularity of the grating [37]. In addition, the mechanical stress effects that accompany the creation of such a grating in the method suggested strongly interfere with the purely geometrical ones and can alter the picture of light propagation in such fiber gratings. From a computational point of view, the expression (1) comprises a phenomenological parameter r_b, whose order is very difficult to assess, nothing to speak of its precise evaluation within the frameworks of the model. This makes theoretical evaluation of the grating performance in a sense unreliable. Moreover, at present this method of creation of HCFs seems to be obsolete. Drawing a HCF from a perform with an off-centered core allows more effective control of the helix parameters [35,38,39]. A schematic view of the HCF obtained by this method is given in Fig. 1.

The HCFs produced by drawing are characterized by the refractive index distribution other than given by Eq. (1). For the step-index fiber the plots of n in the transverse cross section for the described models are represented in Fig. 2. As is obvious, for perform-drawn HCFs the analytical treatment suggested in Ref. [36] is no longer suitable. A natural way seems to be using the helical coordinates (r,φ,s) (Fig. 3). Connection between these coordinates and the Cartesian ones is given by [40]

$$x = R\cos Ks - r\cos\phi\cos Ks + rv\sin\phi\sin Ks,$$

$$y = R\sin Ks - r\cos\phi\sin Ks - rv\sin\phi\cos Ks,$$

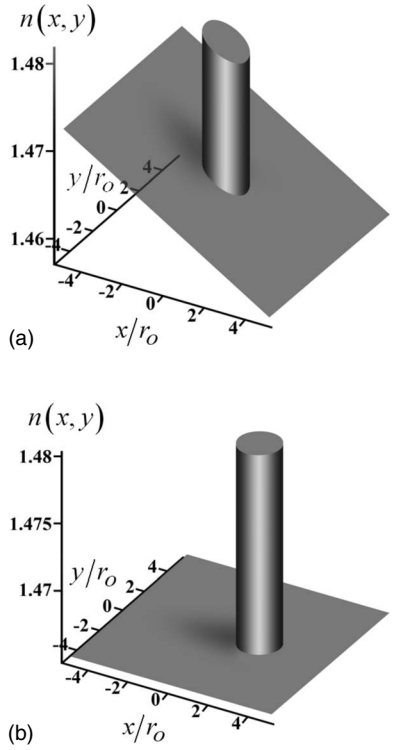

FIG. 2. Refractive index distribution in the transverse cross section $z=0$ for the models of (a) helical core-step-index fiber produced by drawing from a perform; (b) helical core fiber produced by bending the ideal step-index fiber. The fibers' parameters are (a) $n_{co}=1.48$, $\Delta=0.01$, $R=1.5r_0$; (b) $n_{co}=1.48$, $\Delta=0.01$, $r_b=10^3r_0$.

$$z = \upsilon s + rRK \sin\varphi. \tag{2}$$

Here $K=2\pi/[H^2+(2\pi R)^2]^{1/2}$, $\upsilon=HK/2\pi$, R is offset and H is the helix pitch. In these coordinates the vector wave equation in the electric field $\mathbf{E}$ [41]:

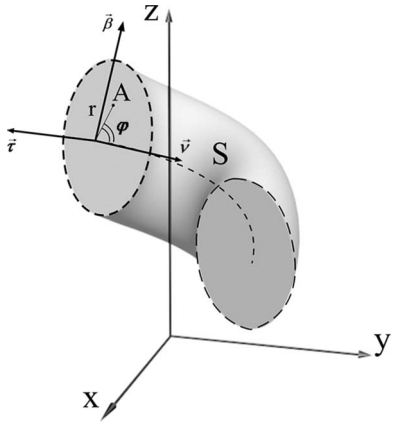

FIG. 3. Local helical coordinates (r,φ,s) in the Frenet frame $\boldsymbol{\nu},\boldsymbol{\beta},\boldsymbol{\tau}$, where $\boldsymbol{\nu}$ is the unit vector of the principal normal, $\boldsymbol{\beta}$ is the unit vector of the binormal, $\boldsymbol{\tau}$ is the unit vector in the tangent direction.

$$[\vec{\nabla}^2 + k^2 n^2(x,y,z)]\mathbf{E}(x,y,z) = -\vec{\nabla}[\mathbf{E}(x,y,z)\cdot\vec{\nabla}\ln n^2(x,y,z)], \tag{3}$$

where $n^2(x,y,z)=n_{co}^2[1-2\Delta f(x,y,z)]$, $\Delta=(n_{co}^2-n_{cl}^2)/2n_{co}^2$, n_{co}, and n_{cl} are the values of the refractive index in the core and cladding, respectively, $\vec{\nabla}=(\partial/\partial x,\partial/\partial y,\partial/\partial z)$, $k=2\pi/\lambda$, and λ is the wavelength, can be written with the help of the standard formulas of differential geometry [42]. First, one has to use the relation for an arbitrary vector field $\mathbf{A}$:

$$\vec{\nabla}^2\mathbf{A} = \vec{\nabla}\vec{\nabla}\cdot\mathbf{A} - \vec{\nabla}\times\vec{\nabla}\times\mathbf{A}, \tag{4}$$

in which the differential operators have to be recast using the known relations

$$\mathrm{div}\mathbf{A} = \frac{1}{\sqrt{G}}\frac{\partial}{\partial x^i}\left(A_i\sqrt{\frac{G}{g_{ii}}}\right), \quad (\vec{\nabla}\Phi)_k = \sqrt{g_{kk}}g^{ki}\frac{\partial\Phi}{\partial x^i},$$

$$(\vec{\nabla}\times\mathbf{A})_i = \sqrt{\frac{g_{ii}}{G}}\left[\frac{\partial}{\partial x_j}\left(g_{kn}\frac{A_n}{\sqrt{g_{nn}}}\right) - \frac{\partial}{\partial x_k}\left(g_{jn}\frac{A_n}{\sqrt{g_{nn}}}\right)\right]. \tag{5}$$

Here

$$g_{ij} = \begin{pmatrix} 1 & 0 & 0 \\ 0 & r^2 & r^2\upsilon \\ 0 & r^2\upsilon & g_{33} \end{pmatrix}$$

is the metric tensor, $g_{33}=(1-r\kappa\cos\varphi)^2+r^2\upsilon^2$, $G=\det g_{ik}$, $\kappa=\frac{4\pi^2R}{H^2+(2\pi R)^2}$ is the curvature of the central line of the fiber, $\upsilon=\frac{2\pi H}{H^2+(2\pi R)^2}$ is its torsion, "det" stands for determinant. In the expression for $\vec{\nabla}$ $(i,j,k)=(1,2,3)$ and all their circular permutations.

The equations in E_r, E_φ, E_s essentially simplify for the weakly coiled fiber approximation, at which $r_0\kappa\ll 1$ (r_0 is the core's radius) [43]. Also at $\Delta\ll 1$ one can disregard the coupling between transversal components $E_{r,\varphi}$ and the longitudinal component E_s. The latter condition, generally speaking, ensures a paraxial propagation of light in waveguides and usually makes it possible to disentangle longitudinal and transversal field components [44]. It is remarkable that despite small offset value ($R\propto r_0$) the pitch of the studied helical grating proves to be such that the condition of weak coiling is still justified. In addition, we will also disregard the term on the right of Eq. (3). This term is essential for the coupling of modes with the same orbital number l [41], but its influence on the process of conversion of modes with different l is negligible. In this way, the waveguide equation will be treated in the scalar approximation. The approximations made enable us to essentially simplify the set of equations in electric field components, which otherwise would have looked much more cumbersome. Since the obtained equations prove to be translation invariant in s, their solutions can be factorized as $\mathbf{E}_{r,\varphi}(r,\varphi,s)=\mathbf{e}_{r,\varphi}(r,\varphi)\exp(i\beta s)$, where β is some propagation constant.

In a matrix form the obtained set of equations in transversal components can be written as

$$(\hat{H}_0 + \hat{V}_0 + \hat{V}_1 + \cdots)|\Phi\rangle_h = \beta^2|\Phi\rangle_h, \tag{6}$$

where $|\Phi\rangle_h \equiv \begin{pmatrix} e_r(r,\varphi) \\ e_\varphi(r,\varphi) \end{pmatrix}$ and $\mathbf{e}_{r,\varphi}$ are the components in the local basis $\mathbf{n}_r$, $\mathbf{n}_\varphi$, which is specified by the subscript h. The operator $\hat{H}_0$ describes the propagation of light in a straight ideal fiber (in the local basis of cylindrical-polar coordinates):

$$\hat{H}_0 = \left(\frac{\partial^2}{\partial r^2} + \frac{1}{r}\frac{\partial}{\partial r} + \frac{1}{r^2}\frac{\partial^2}{\partial \varphi^2} - \frac{1}{r^2} + k^2\tilde{n}^2(r)\right)\hat{\sigma}_0 + \frac{2i}{r^2}\frac{\partial}{\partial \varphi}\hat{\sigma}_2, \tag{7}$$

where $\hat{\sigma}_i$ is the Pauli matrix. The perturbation operators $\hat{V}_i$ are obtained as decomposition over certain small parameters and have the form

$$\hat{V}_0 \approx -2i\beta\upsilon\vec{\nabla}_\varphi, \tag{8}$$

$$\hat{V}_1 \approx -2r\kappa\beta^2\cos\varphi. \tag{9}$$

The perturbation operator is organized in such *a* way as to separate the terms that in effect provide coupling between the groups of modes, which have the same difference between the total angular momentum numbers $M = l + \sigma$. So, the operator $\hat{V}_i$ couples the modes with $|\Delta M| = i$. In Eqs. (8) and (9) we have retained only the main terms of the decompositions. Analogously, in Eq. (6) we have restricted our consideration to the cases $i = 0, 1$, although, in principle, i has no upper limit. Equation (6) is the desired waveguide equation in the helical coordinates.

III. RESONANCE MODE COUPLING

Mathematically, Eq. (6) is an eigenvalue equation with a pronounced hierarchy of small parameters, so it can be solved using the methods of perturbation theory [45]. As is easily demonstrated, at $|l| \geqslant 1$ the spectrum of the zero-approximation equation $\hat{H}_0|\Phi\rangle_h = \tilde{\beta}_l^2|\Phi\rangle_h$, where $\tilde{\beta}_l$ is the scalar propagation constant, is fourfold degenerate. There are four eigenvectors that correspond to the eigenvalue $\tilde{\beta}_l^2$ [46]:

$$|1,l\rangle_h = e^{i(l+1)\phi}\begin{pmatrix} 1 \\ i \end{pmatrix}F_l(r), \quad |1,-l\rangle_h = e^{i(1-l)\phi}\begin{pmatrix} 1 \\ i \end{pmatrix}F_l(r),$$

$$|-1,-l\rangle_h = e^{i(-l-1)\phi}\begin{pmatrix} 1 \\ -i \end{pmatrix}F_l(r), \quad |-1,l\rangle_h = e^{i(l-1)\phi}\begin{pmatrix} 1 \\ -i \end{pmatrix}F_l(r), \tag{10}$$

where the radial function $F_l(r)$ satisfies the equation [41]

$$\left(\frac{\partial^2}{\partial r^2} + \frac{1}{r}\frac{\partial}{\partial r} + k^2\tilde{n}^2(r) - \frac{l^2}{r^2} - \tilde{\beta}^2\right)F_l(r) = 0. \tag{11}$$

In the Frenet basis $\boldsymbol{\nu}$, $\boldsymbol{\beta}$ (see Fig. 3) the same vectors have a more recognizable form of circularly polarized OVs with topological charge $\pm l$:

$$|1,l\rangle = e^{il\phi}\begin{pmatrix} 1 \\ i \end{pmatrix}F_l(r), \quad |1,-l\rangle = e^{-il\phi}\begin{pmatrix} 1 \\ i \end{pmatrix}F_l(r),$$

$$|-1,-l\rangle = e^{-il\phi}\begin{pmatrix} 1 \\ -i \end{pmatrix}F_l(r), \quad |-1,l\rangle = e^{il\phi}\begin{pmatrix} 1 \\ -i \end{pmatrix}F_l(r). \tag{12}$$

Here the first index of a ket vector stands for polarization and the second index indicates its topological charge. In what follows we will present the final expressions written in the Frenet frame, though all the calculations are carried out in the local helical basis. Here and throughout the absence of subscript at a vector means its representation over the Frenet frame $|\Phi\rangle \equiv \begin{pmatrix} e_\nu(r,\varphi) \\ e_\beta(r,\varphi) \end{pmatrix}$.

Whereas for straight fibers the eigenvalues $\tilde{\beta}_l^2$ are degenerate, at nonzero torsion the spectrum branches, which correspond to OVs with different topological charge, are well spaced. To study this effect consider the first-order corrections to the scalar propagation constant. In our case the largest contribution is given by the operator $\hat{V}_0$. Since $|\sigma,l\rangle = e^{i(l+\sigma)\varphi}\begin{pmatrix} 1 \\ i\sigma \end{pmatrix}F_l(r)$, if one defines the scalar product as

$$\langle\Phi|\Psi\rangle = \int_0^\infty \int_0^{2\pi} (\Phi_r^* \ \Phi_\varphi^*)\begin{pmatrix} \Psi_r \\ \Psi_\varphi \end{pmatrix} r dr d\varphi, \tag{13}$$

the correction to $\tilde{\beta}_l$ that corresponds to the forward-propagating zero-approximation solution $|\sigma,l\rangle$ can be found:

$$\Delta\beta_{\sigma,l} = (\sigma + l)\upsilon. \tag{14}$$

This remarkably simple result describes the topological effect that accompanies propagation of OVs along curved trajectories [47]. In addition to the term $\sigma\upsilon$ that corresponds to Berry's phase of spinning photons, it also comprises the contribution $l\upsilon$, which arises due to photon's intrinsic OAM. The latter term is essentially the manifestation of the so-called orbit-orbit interaction. The effect of such topologically induced corrections is twofold. First, the initial degeneracy is partially (or completely, as for $l=0$ and $l>1$ modes) lifted. Secondly, for certain values of torsion υ another kind of degeneracy may appear. Indeed, in Fig. 4 the torsion-induced splitting of "energy levels" is shown for $l=0,1$ spectral branches. Since

$$\beta_{\sigma,l}(\upsilon) = \tilde{\beta}_l + (\sigma + l)\upsilon, \tag{15}$$

υ coordinates of the intersection points (a) and (b) prove to be the same: $\upsilon_a = \upsilon_b = \tilde{\beta}_1 - \tilde{\beta}_0$, whereas $\upsilon_c = \upsilon_a/3$. In these points of the so-called accidental degeneracy there may occur the coupling of the corresponding zero-approximation modes $|\sigma,l\rangle$. Note that the branch that corresponds to $|1,-1\rangle$, $|-1,1\rangle$ OVs remain double degenerate. As is known, this degeneracy is lifted by the gradient term on the right of Eq. (3) [41], however, we disregard this effect.

Near these points it is necessary to take account of the higher-order perturbation operators $\hat{V}_i$ to lift the degeneracy. It should be emphasized that in such points a type of coupling becomes possible that hybridizes the modes with different orbital numbers. Such coupled modes strongly interact with each other enabling various processes of energy redistribution from one of the modes to another. Such situation is usually described within the frameworks of the coupled

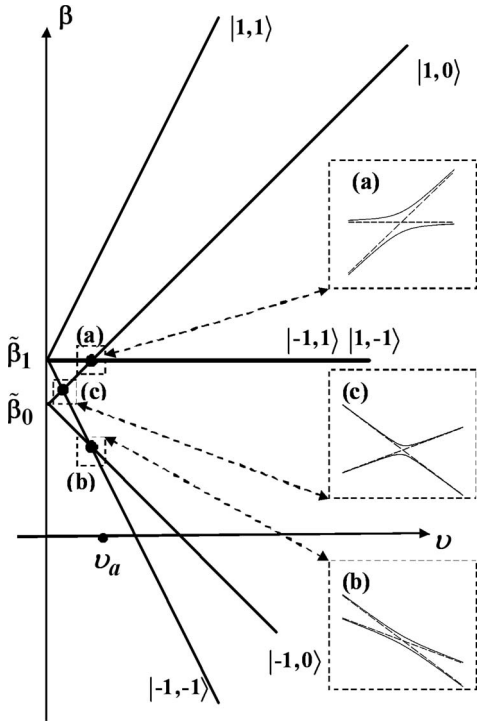

FIG. 4. Torsion-induced splitting of "energy levels" $\beta_{\sigma,l}(\upsilon)$ for $l=0,1$ zero-approximation modes $|\sigma,l\rangle$. The type of the mode is indicated near the spectral branch. Positions of the intersection points (a)–(c) where the mode conversion takes place are marked with black dots. Insets show repulsion of spectral curves due to hybridization of corresponding modes.

mode theory; however, this can be also done using the perturbation theory. To do this one has to build the matrix H of the total Hamiltonian $\hat{H}_0+\Sigma\hat{V}_i$ over the states that represent the converging spectral branches and solve the eigenvalue problem for the obtained matrix [36]. In our case the largest operator, which provides the desired coupling of modes with $\Delta M=1$, is $\hat{V}_1$. Comparison with the model of bend-induced HCFs [36], in which a helicoidal bending gives rise to the analogous perturbation term $-2\frac{r}{r_b}k^2\tilde{n}^2\cos\varphi$, establishes complete coincidence of the corresponding perturbation operators at $r_b=1/\kappa$. In this way a phenomenological bend parameter r_b, introduced in Ref. [36], is analogous to the curvature radius of the helix in our model.

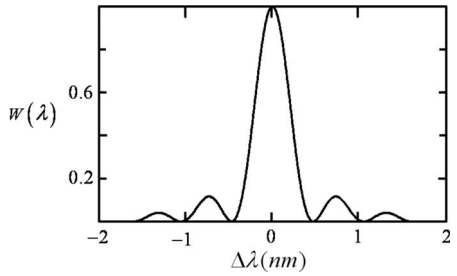

FIG. 5. The energy W stored in the vortex vs wavelength detuning $\Delta\lambda=\lambda-\lambda_0$ in the process of conversion of the fundamental mode into the OV. The fiber length is optimal: $s=s_0$; other fiber parameters are $\Delta=0.03$, $r_0=6.323$ μm, $R=0.5r_0$, $H=0.18$ mm, λ_0 is the wavelength of a He-Ne laser.

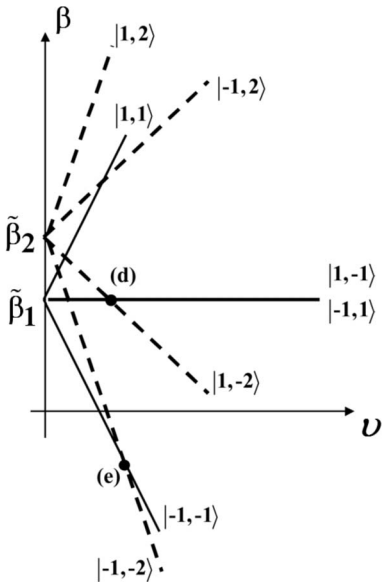

FIG. 6. Torsion-induced splitting of spectral branches for $l=1,2$ zero-approximation vortex modes. Positions of the intersection points (d)–(e), where the mode conversion takes place are marked with black dots.

This analogy enables us to take advantage of some of results obtained in Ref. [36] concerning the coupling of forward-propagating modes. Near (a) the eigenvalue equation for the matrix H built over the vectors $|1,0\rangle$ and $|1,-1\rangle$ has the form analogous to Eq. (17) of Ref. [36]:

$$\begin{pmatrix} \tilde{\beta}_0^2-(\beta-\upsilon)^2 & A \\ A & \tilde{\beta}_1^2-\beta^2 \end{pmatrix}\mathbf{x}_a=0, \tag{16}$$

where $\mathbf{x}_a=(a,b)^T$ stands for the field $|\Psi\rangle=a|1,0\rangle+b|1,-1\rangle$. The coupling constant is given by $A=r_0\kappa k^2n_{co}^2\int_0^\infty x^2F_0(x)F_1(x)dx/\sqrt{N_0N_1}$, where the normalization factor is defined as $N_i=\int_0^\infty xF_i^2(x)dx$. Decomposition of Eq. (16) near the point $(\tilde{\beta}_1-\tilde{\beta}_0,\tilde{\beta}_1)$ gives, in the same manner, the modification of the spectral dependence

$$\beta_{1,2}=\tilde{\beta}_1-\tilde{\beta}_0+\frac{1}{2}[\upsilon-\upsilon_a\pm\sqrt{(\upsilon-\upsilon_a)^2+Q^2}], \tag{17}$$

where $Q\approx A/\tilde{\beta}$ (it is assumed that for weakly guiding fibers $\tilde{\beta}_1\approx\tilde{\beta}_0\approx\tilde{\beta}$). The spectra (20) also feature the so-called repulsion of energy levels [45]. The hybrid modes have the form

$$|\Psi_{1a}\rangle=C_+|1,0\rangle+C_-|1,-1\rangle,\quad |\Psi_{2a}\rangle=C_-|1,0\rangle-C_+|1,-1\rangle, \tag{18}$$

where $C_\pm=\frac{1}{\sqrt{2}}\sqrt{1\pm\mathrm{sgn}(\upsilon-\upsilon_a)[1+Q^2/(\upsilon-\upsilon_a)^2]^{-1/2}}$.

It is sometimes necessary to have the expressions for modes in the laboratory Cartesian frame. This, generally,

rather cumbersome transition, can be easily done in our particular case. Indeed, since $R \propto r_0$ and near the intersection point $H \propto (\tilde{\beta}_1 - \tilde{\beta}_0)^{-1}$, one has $H \gg R$, so that the tangent vector $\boldsymbol{\tau}$ is almost parallel to the z axis. Therefore, approximately, the Frenet frame merely rotates about the z axis. The rotation angle γ linearly depends on z:

$$\gamma = \frac{2\pi}{H} z, \tag{19}$$

where z is the coordinate of the point on the central line of the helical core. This leads to the following connection between the azimuthal angle φ_F measured in the Frenet frame and the corresponding angle φ_C measured in the Cartesian frame $\varphi_F = \varphi_C - \gamma - \pi$. Finally, the expression for an OV $|\sigma, l\rangle_F$ written in the Frenet frame can be represented through the expression for the same OV $|\sigma, l\rangle_C$ given in the Cartesian frame, as

$$|\sigma, l\rangle_F = |\sigma, l\rangle_C e^{-i(\sigma+l)(\gamma+\pi)}. \tag{20}$$

Of course, the vector $|\sigma, l\rangle_C$ should depend on φ_C, which is achieved by a formal substitution in Eq. (13): $\varphi \to \varphi_C$. In addition, it is also necessary to pass everywhere in the phase exponentials $\exp(i\beta s)$ to the z coordinate using the connection

$$z = \frac{Hs}{\sqrt{H^2 + (2\pi R)^2}}. \tag{21}$$

Expressions (19)–(21) should be used for the transition to the Cartesian basis. Of course, certain modifications should also be made in the radial functions $F_l(r)$ allowing for the shift of origin: $r \to r + R$. However, the latter transformation is not that crucial as the transformations over the phase dependence of the modes and is quite obvious.

In the same manner, one can treat the mode hybridization, which takes place near the point (b), where the partial fields $|-1, 0\rangle$ and $|-1, -1\rangle$ get coupled. The resulting eigenvalue equation reads

$$\begin{pmatrix} \tilde{\beta}_0^2 - (\beta + \upsilon)^2 & A \\ A & \tilde{\beta}_1^2 - (\beta + 2\upsilon)^2 \end{pmatrix} \mathbf{x}_b = 0, \tag{22}$$

where $\mathbf{x}_b = \mathrm{col}(a, b)$ stands for $|\Psi\rangle = a|-1, 0\rangle + b|-1, -1\rangle$. The spectra are described by the following expressions:

$$\beta_{3,4} = 2\tilde{\beta}_0 - \tilde{\beta}_1 + \frac{1}{2}[-3(\upsilon - \upsilon_a) \pm \sqrt{(\upsilon - \upsilon_a)^2 + Q^2}], \tag{23}$$

which also feature repulsion of spectral branches. Modes in the Frenet frame are

$$|\Psi_{3b}\rangle = C_+|-1, 0\rangle + C_-|-1, -1\rangle,$$

$$|\Psi_{4b}\rangle = C_-|-1, 0\rangle - C_+|-1, -1\rangle. \tag{24}$$

In this model of a HCF one additional type of mode coupling is possible: the coupling between $|-1, -1\rangle$ OV and the fundamental mode $|1, 0\rangle$, which occurs near the point (c). However, the operators $\hat{V}_0, \hat{V}_1$ [see Eqs. (8) and (9)] prove unable to provide this kind of coupling. One has to study the next terms of decomposition into $\hat{V}_i$. One can show that the desired coupling is provided by the operator $\hat{V}_3$. The main term that contributes to this effect can be represented as

$$\hat{V}_3 \approx \frac{1}{2} \cos\varphi \sin 2\varphi r \kappa^3 \begin{pmatrix} 0 & 1 \\ 0 & 0 \end{pmatrix}. \tag{25}$$

Being combined with $\hat{V}_0$, this operator generates the following matrix equation:

$$\begin{pmatrix} \tilde{\beta}_0^2 - (\beta - \upsilon)^2 & U \\ U & \tilde{\beta}_1^2 - (\beta + 2\upsilon)^2 \end{pmatrix} \mathbf{x}_c = 0. \tag{26}$$

Here $U = r_0 \kappa^3 \int_0^\infty x^2 F_0(x) F_1(x) dx / \sqrt{N_0 N_1}$ and the vector $\mathbf{x}_c = \mathrm{col}(a, b)$ stands for the field $|\Psi\rangle = a|1, 0\rangle + b|-1, -1\rangle$. This resonance occurs at $\upsilon_c = \frac{1}{3}\upsilon_a$. The repulsion of spectral curves is described by

$$\beta_{3,4} = \frac{1}{3}(2\tilde{\beta}_0 + \tilde{\beta}_1) + \frac{1}{2}[-(\upsilon - \upsilon_c) \pm \sqrt{9(\upsilon - \upsilon_c)^2 + \tilde{Q}^2}], \tag{27}$$

where $\tilde{Q} = U/\tilde{\beta}$. The structure of hybrid modes near this point is described by analogous expressions

$$|\Psi_{5c}\rangle = \tilde{C}_+|1, 0\rangle - \tilde{C}_-|-1, -1\rangle,$$

$$|\Psi_{6c}\rangle = \tilde{C}_-|1, 0\rangle + \tilde{C}_+|-1, -1\rangle, \tag{28}$$

where $\tilde{C}_\pm = \frac{1}{\sqrt{2}} \sqrt{1 \pm \mathrm{sgn}(\upsilon - \upsilon_c)[1 + \tilde{Q}^2/(3\upsilon - 3\upsilon_c)^2]^{-1/2}}$. Note that since near the intersection point $\frac{U}{A} = \frac{r_0^2(\tilde{\beta}_1 - \tilde{\beta}_0)^2}{k^2 n_{co}^2} << 1$, the width of the effective coupling zone in this case is much less than for previously considered cases.

IV. GENERATION AND TRANSFORMATIONS OF OPTICAL VORTICES

Topologically induced coupling between fiber modes leads to energy exchange between the constituting fields, which is manifested in mode conversion. The most practically important type of such conversion is the transformation of the fundamental modes into OVs. Consider, as an example, conversion of the $|1, 0\rangle$ mode into the OV $|1, -1\rangle$. If at the input end ($s = 0$) of the HCF one excites the fundamental mode $|1, 0\rangle$ (details of the experimental technique can be found in [31]) then it evolves in the fiber as

$$|\Phi(s)\rangle = \left\{ \left[\cos(0.5s\sqrt{\varepsilon^2 + Q^2}) + \frac{i\varepsilon}{\sqrt{\varepsilon^2 + Q^2}} \sin(0.5s\sqrt{\varepsilon^2 + Q^2}) \right] |1, 0\rangle + \frac{iQ}{\sqrt{\varepsilon^2 + Q^2}} \sin(0.5s\sqrt{\varepsilon^2 + Q^2}) |1, -1\rangle \right\} \times \exp[i(\tilde{\beta}_1 + 0.5\varepsilon)s], \tag{29}$$

where $\varepsilon=\upsilon-\upsilon_a$. The structure of this expression has much in common with the corresponding formula for LP_{01} mode conversion obtained in Ref. [31] with the coupled mode theory. However, there is no detailed coincidence since in Eq. (29) the local basis is used. Complete transformation of $|1,0\rangle$ mode into $|1,-1\rangle$ OV takes place at $\varepsilon=0$, or at $\upsilon=\tilde{\beta}_1-\tilde{\beta}_0$. In this case at $s_n=(2n+1)\pi/Q$ the cosine term vanishes and $|\Phi(s_n)\rangle\propto|1,-1\rangle$. The last relation conveys the conversion of the fundamental mode into the OV with topological charge −1. For example, for a fiber with $n_{co}=1.48$, $\Delta=0.01$, and $R=1.5r_0$ one has $s_0=4.2\times10^{-4}$ m.

Effectiveness of the energy transformation into the vortex state in this case is 100%, however, it is true only for a unique wavelength of the incident beam, at which $\varepsilon(\lambda)=0$. If this does not take place, for a constant torsion of the helix the $|1,0\rangle$ mode would not be totally converted into the vortex by the fiber. The energy W (in relative units) stored in the vortex is

$$W=\frac{Q^2}{\varepsilon^2+Q^2}\sin^2(0.5s\sqrt{\varepsilon^2+Q^2}). \tag{30}$$

For a fiber of an optimal length (for example, $s=s_0$) the energy of the output vortex changes with ε as

$$W(\varepsilon,s=s_0)=\frac{Q^2}{\varepsilon^2+Q^2}\sin^2\left(\frac{\pi}{2Q}\sqrt{\varepsilon^2+Q^2}\right). \tag{31}$$

Although it is natural to describe this process in terms of detuning ε, experimentally, one not always has the ability to change the value of helix's torsion for the prepared HCF. Such may be the case where the fiber is used as a torsion or temperature sensor, for example. In other cases, especially where a broadband source of light is used, the fiber parameters are assumed to be constant, whereas the wavelength changes. In these cases one can describe the HE_{11} mode transformation through transmittance spectrum. If at certain wavelength λ_0 the fiber totally transforms the fundamental mode into an OV, i.e., $s=s_n$, the energy imparted to the vortex at the other wavelength will be

$$W(\lambda)=\frac{Q^2}{\varepsilon^2(\lambda)+Q^2}\sin^2\left(\pi\left(n+\frac{1}{2}\right)\sqrt{1+\frac{\varepsilon^2(\lambda)}{Q^2}}\right), \tag{32}$$

where $\varepsilon(\lambda)=[\tilde{\beta}_1(\lambda_0)-\tilde{\beta}_1(\lambda)]-[\tilde{\beta}_0(\lambda_0)-\tilde{\beta}_0(\lambda)]$. The conversion characteristics for n=0 is given in Fig. 5. If the fiber length is not optimal at λ_0, the conversion would be less effective.

This situation is quite the same for conversion of $|-1,0\rangle$ mode into the OV $|-1,-1\rangle$, which occurs near (b). Since $\upsilon_b=\upsilon_a$ the HCF can equally effective perform both these transformations, that is the conversion performance is polarization insensitive. The third type of conversion, which takes place near (c), for a fiber with constant parameters will be registered at another wavelength as a narrow peak in OV generation (or a deep in HE_{11} mode transmission). For a fixed wavelength since $\upsilon_c=\upsilon_a/3$ the pitch of the core's helix should be tripled to satisfy the resonance condition. As is obvious from these examples, in the resonance area the fiber lowers the value of the topological charge of the incident beam by 1. For the opposite core's helicity the charge of the beam would be increased by 1. In this way such fibers enable operation with the topological charge of the signal, which might be useful for information purposes.

Quite analogously, such fibers can transform the topological charge of $l=1$ OVs. To demonstrate this, consider the coupling of $l=1$ and $l=2$ OVs. In the zero approximation the spectral curves have the form $\beta(\upsilon)=\tilde{\beta}_{1,2}+(l+\sigma)\upsilon$ (see Fig. 6). Mode conversion can occur only in the intersection points, however, the most effective conversion is provided by the operator $\hat{V}_1$ given by Eq. (9), which couples the OVs with the same polarization and $\Delta l=1$. So, effective mode coupling takes place only in the points (d) and (e). The corresponding eigenvalue equation for these points has the form

$$\begin{pmatrix}\tilde{\beta}_1^2-\beta^2 & G\\ G & \tilde{\beta}_2^2-(\beta+\upsilon)^2\end{pmatrix}\mathbf{x}_d=0 \tag{33}$$

and

$$\begin{pmatrix}\tilde{\beta}_1^2-(\beta+2\upsilon)^2 & G\\ G & \tilde{\beta}_2^2-(\beta+3\upsilon)^2\end{pmatrix}\mathbf{x}_e=0, \tag{34}$$

where $\mathbf{x}_d$ belongs to the space spanned over $|1,-1\rangle$ and $|1,-2\rangle$ vectors and $\mathbf{x}_e$ is decomposed over $|-1,-1\rangle$ and $|-1,-2\rangle$ OVs. The coupling constant is $G=-\frac{r_0\kappa k^2 n_{co}^2}{8\sqrt{N_1N_2}}\int_0^\infty x^2F_1(x)F_2(x)dx$. In the same manner one can show that the structure of hybrid modes is given by the formulas analogous to Eqs. (18), (24), and (28). Naturally, such hybridization also implies conversion of OVs, whose length for optimal torsion $\upsilon_{d,e}$ is

$$\upsilon_d=\upsilon_e=\tilde{\beta}_2-\tilde{\beta}_1, \tag{35}$$

is determined as $s_n=(2n+1)\pi\tilde{\beta}/G$. Typical values of conversion length in this case for weakly guiding fibers are less than one millimeter. So, for a fiber with $n_{co}=1.48$, $\Delta=0.01$, and $R=1.5r_0$ one has $s_0=2\times10^{-4}$ m. It is interesting to note that, according to the above analysis, at different values of torsion parameter υ the fiber may differently react to the input beam. So, at $\upsilon=\upsilon_a$ the fiber would transform the incident $|1,-1\rangle$ vortex into the fundamental mode $|1,0\rangle$, whereas at $\upsilon=\upsilon_d$ the same OV would be converted into the higher-order OV $|1,-2\rangle$. In the same way such fibers can change by unity topological charges of OVs with higher orbital numbers. Of course, the fiber has to support the propagation of modes with large enough values of l, that is, the waveguide parameter should enable guided propagation of generated higher-order vortex. For example, to generate an OV from the fundamental mode one should use the fiber with $V>2.4$; charge-2 OV can be generated in fibers with $V>3.8$, and so on.

Analysis shows, that intermodal conversions can affect both orbital and spin state of the input mode. The nature of this transformation strongly depends on the explicit form of the coupling operator $\hat{V}_i$. If this operator affects only the orbital state, as in the case of $\hat{V}_1$ operator, the polarization state of the transforming mode would not be changed. Ex-

amples of such behavior are provided by the coupling near the points (a) and (b) on Fig. 4. Such transformations do not involve spin-orbit coupling (not presented in the operator $\hat{V}_1$), therefore one cannot control the state of the OAM of the outgoing beam by flipping the spin of the incoming field. In contrast to $\hat{V}_1$ the operator $\hat{V}_3$ changes both spin and orbital state of a vector, thus providing near the point (c) (Fig. 4) the transformation of spin and orbital AM of the incoming beam. However, since the point (c) does not have any "counterpart," such as, say, point (a), this effect also cannot be used for controlling the orbital state through the spin state control.

It should be stressed that the coupling of partial fields $|\sigma_i, l_i\rangle$ and $|\sigma_k, l_k\rangle$ occurs if the torsion satisfies the condition

$$\tilde{\beta}_i - \tilde{\beta}_k = (M_k - M_i)\upsilon, \tag{36}$$

which should be treated as a generalization of an ordinary coupling condition $\beta_i - \beta_k = q$ that is fulfilled in straight fibers for the grating with the lattice vector q. In our case, being induced by a topological effect, this coupling is sensitive to the index M of the mode's total angular momentum.

The final remark concerns modifications of the obtained results for different relations between the scalar propagation constants. For simplicity we have assumed that $\beta_0 < \beta_1$ and $\beta_1 < \beta_2$. If one of these relations is wrong, one can show that in the corresponding expressions for mode coupling one has to invert the signs of indices in all the ket vectors: $|\sigma, l\rangle \rightarrow |-\sigma, -l\rangle$. Basically, this is connected with the fact that the ordering of β assumed in this paper is restored by inversion of the β axis in Figs. 4 and 6, with simultaneous reflection of spectral curves about the υ axis. The latter is achieves just by the abovementioned sign inversion.

V. EFFECT OF CORE'S ELLIPTICITY ON THE SPLITTING OF RESONANCES

As follows from the results of the previous section, there are two kinds of conversions associated with each resonance torsion or wavelength, which are related to transformations of oppositely polarized incident beams. This property of the system is somewhat desirable since it enables conversion of linearly polarized beams, which can be considered as a superposition of circularly polarized fields. However, as was mentioned in Ref. [35], while manufacturing the HCFs the custom fiber perform, which the fiber is drawn from, have an eccentric elliptical core. It is therefore desirable to study the influence of ellipticity on mode transformations in HCFs.

Within the frameworks of our model, the easiest way to introduce ellipticity is to add to the left-hand side of Eq. (6) the following term [46]:

$$\hat{V}_{\text{ell}} = -2k^2 n_{\text{co}}^2 \Delta\, \delta r \tilde{f}_r' \cos 2\varphi \hat{\sigma}_0, \tag{37}$$

where $\delta \ll 1$ is the parameter of ellipticity connected with the ellipse's eccentricity e as $e = 2\sqrt{\delta}/(1+\delta)$. This term is obtained through decomposition of elliptically deformed profile function $\tilde{f}(x(1+\delta), y(1-\delta))$, where $\tilde{f}(x,y) = f(r)$. It is easily verified that since $\hat{V}_{\text{ell}}$ couples OVs with the same polarization and $\Delta l = 2$, it gives zero contribution to the eigenvalue equations (16), (22), (26), and (33). However, it is possible to modify the previously used effective scheme of obtaining those equations to include the effect of ellipticity.

Following Ref. [36], consider the matrix H of the total Hamiltonian $\hat{H}$ built over the vectors

$$|1\rangle = |1,0\rangle, |2\rangle = |-1,0\rangle, |3\rangle = |1,1\rangle, |4\rangle = |1,-1\rangle, 5 = |-1,-1\rangle, |6\rangle = |-1,1\rangle. \tag{38}$$

The eigenvalue equation that corresponds to this matrix is

$$\begin{pmatrix} \tilde{\beta}_0^2 - (\beta - \upsilon)^2 & 0 & A & A & 0 & 0 \\ 0 & \tilde{\beta}_0^2 - (\beta + \upsilon)^2 & 0 & 0 & A & A \\ A & 0 & \tilde{\beta}_1^2 - (\beta - 2\upsilon)^2 & D & 0 & 0 \\ A & 0 & D & \tilde{\beta}_1^2 - \beta^2 & 0 & 0 \\ 0 & A & 0 & 0 & \tilde{\beta}_1^2 - (\beta + 2\upsilon)^2 & D \\ 0 & A & 0 & 0 & D & \tilde{\beta}_1^2 - \beta^2 \end{pmatrix} \mathbf{x} = 0, \tag{39}$$

where the ellipticity-induced constant reads for a step-index fiber $D = -k^2 n_{\text{co}}^2 \Delta\, \delta F_1^2(r = r_0)/N_1$. To reduce this equation to the previously considered case it is proposed to make a partial diagonalization of H so that 2×2 matrix blocks $\hat{H}_{ii}$ that stand on the principal diagonal of the corresponding block matrix become diagonal. Such diagonalizing matrix has the form

$$\hat{S} = \begin{pmatrix} \hat{1} & \hat{0} & \hat{0} \\ \hat{0} & \hat{C}_2 & \hat{0} \\ \hat{0} & \hat{0} & \hat{C}_3 \end{pmatrix}, \tag{40}$$

where $\hat{C}_i$ diagonalizes matrix blocks $\hat{H}_{ii}$, so that if H is represented as

$$H=\begin{pmatrix}\hat{H}_{11} & \hat{H}_{12} & \hat{H}_{13}\\ \hat{H}_{21} & \hat{H}_{22} & \hat{H}_{23}\\ \hat{H}_{31} & \hat{H}_{32} & \hat{H}_{33}\end{pmatrix}$$

the matrices $\hat{C}_2\hat{H}_{22}\hat{C}_2^{-1}$ and $\hat{C}_3\hat{H}_{33}\hat{C}_3^{-1}$ are diagonal.

To carry out this program, consider diagonalization of the block matrix $\hat{H}_{22}$

$$\hat{C}_2\hat{H}_{22}\hat{C}_2^{-1}=\mathrm{diag}(\lambda_1,\lambda_2), \tag{41}$$

where formal eigenvalues of $\hat{H}_{22}$ are

$$\lambda_{1,2}=\tilde{\beta}_1^2-(\beta-v)^2-v^2\pm\sqrt{4v^2(\beta-v)^2+D^2} \tag{42}$$

(note their dependence on β) and

$$\hat{C}_2=\begin{pmatrix}\dfrac{\beta}{\sqrt{\beta^2-(\lambda_1-\alpha)^2}} & \dfrac{\lambda_1-\alpha}{\sqrt{\beta^2-(\lambda_1-\alpha)^2}}\\ \dfrac{\beta}{\sqrt{\beta^2-(\lambda_2-\alpha)^2}} & \dfrac{\lambda_2-\alpha}{\sqrt{\beta^2-(\lambda_2-\alpha)^2}}\end{pmatrix}, \tag{43}$$

with $\alpha=\tilde{\beta}_1^2-(\beta-2v)^2$. To obtain the zero-approximation spectral curves one has also to solve the equation $\lambda_i(\beta)=0$, which gives for forward-propagating zero-approximation modes

$$\bar{\beta}_{1,2}=v+\sqrt{v^2+\tilde{\beta}_1^2\pm\sqrt{4v^2\tilde{\beta}_1^2+D^2}}. \tag{44}$$

At $D=0$ these curves go over into the straight lines depicted in Fig. 4. Along with the changing of the spectral curves, the form of the basic vectors, which correspond to the spectra (44), also changes. For example, whereas $\hat{H}_{22}$ is built over the basis of purely vortex modes $\binom{|1,1\rangle}{|1,0\ -1\rangle}$, upon diagonalization the basic vectors change for $\hat{C}_2\binom{|1,1\rangle}{|1,0\ -1\rangle}$ and represent in this way certain combinations of OVs. In essence, this transformation corresponds to renormalization of the ground state (zero-order operator) and the transition to the description in terms of "quasi particles" with renormalized dispersion law, which in our case coincide with the modes of twisted elliptical fibers [48].

Being torsion dependent, otherwise rather cumbersome expressions for $\hat{C}_i$ greatly simplify near the intersection points. One can show that at such values of torsion $v_a\tilde{\beta}_1 \gg D$ and the expressions (44) get simplified:

$$\bar{\beta}_{|1,1\rangle}\approx\tilde{\beta}_1+2v+2v_a\xi^2,\quad \bar{\beta}_{|1,-1\rangle}\approx\tilde{\beta}_1-2v_a\xi^2, \tag{45}$$

where $\xi=D/4v_a\tilde{\beta}_1^2$ and the subscript at $\bar{\beta}$ specifies an approximate type of the mode. Comparison with Eq. (15) shows that the presence of ellipticity leads to shifts of spectral curves near intersection points. In the same approximation, one obtains for the diagonalizing matrices

$$\hat{C}_2(\xi)=\hat{C}_3(-\xi)=\frac{1}{\sqrt{1+\xi^2}}\begin{pmatrix}1 & \xi\\ -\xi & 1\end{pmatrix}. \tag{46}$$

Finally, one obtains the desired modification of Eq. (39):

$$\begin{pmatrix}\tilde{\beta}_0^2-(\beta-v)^2 & 0 & A_+ & A_- & 0 & 0\\ 0 & \tilde{\beta}_0^2-(\beta+v)^2 & 0 & 0 & A_- & A_+\\ A_+ & 0 & \tilde{\beta}_1^2-(\beta-2v)^2+\tilde{\beta}\xi & 0 & 0 & 0\\ A_- & 0 & 0 & \tilde{\beta}_1^2-\beta^2-\tilde{\beta}\xi & 0 & 0\\ 0 & A_- & 0 & 0 & \tilde{\beta}_1^2-(\beta+2v)^2+\tilde{\beta}\xi & 0\\ 0 & A_+ & 0 & 0 & 0 & \tilde{\beta}_1^2-\beta^2-\tilde{\beta}\xi\end{pmatrix}\mathbf{x}'=0, \tag{47}$$

where $A_\pm=\frac{1\pm\xi}{\sqrt{1+\xi^2}}$.

Comparing this equation with Eq. (39), one can conclude that ellipticity leads to renormalization of the coupling constant A, which leads to certain change in the width Q of the area, where mode hybridization is essential.

The other effect of elliptic shape of the core is the modification of the basis vectors, over which the matrix $\hat{S}H\hat{S}^{-1}$ is built. For example, the vector $\mathbf{x}'=\mathrm{col}(x_1,\ldots,x_6)$ stands for the field $|\Psi\rangle=x_1|1,0\rangle+x_2|-1,0\rangle+x_3|\psi_3\rangle+x_4|\psi_4\rangle+\cdots$, where

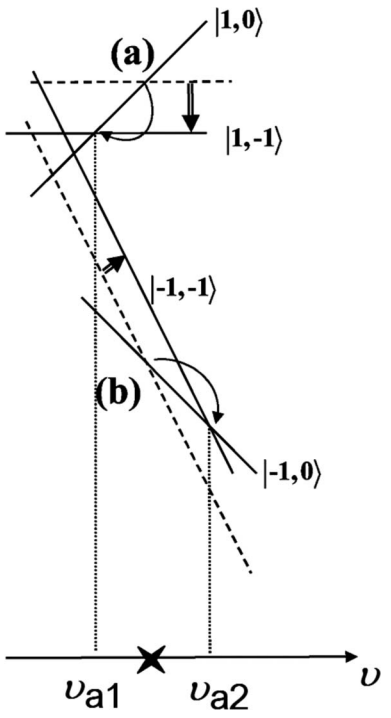

FIG. 7. Splitting of the resonance critical value υ_a (marked by the cross on the υ axis) into υ_{a1} and υ_{a2} critical points for right and left circularly polarized $l=0,1$ coupled modes, respectively. Positions of zero-approximation spectral branches for round-core HCFs are shown in dashed lines. Shifts of zero-approximation branches are indicated with thick arrows; thin arrows show displacement of intersection points (a) and (b) of round-core helical fibers (see Fig. 4).

$$|\psi_3\rangle = k_1|1,1\rangle + k_2|1,-1\rangle, \quad |\psi_4\rangle = -k_2|1,1\rangle + k_1|1,-1\rangle, \tag{48}$$

and $k_1=1/\sqrt{1+\xi^2}$, $k_2=\xi/\sqrt{1+\xi^2}$. This modification, however, is not critical since $\xi \ll 1$ so that one has approximately $|\psi_3\rangle \approx |1,1\rangle$ and $|\psi_4\rangle \approx |1,-1\rangle$, as in the case of a nonperturbed core. The last effect consists in the shift of the spectral curves, given near the intersection points by Eqs. (45). This leads to the splitting of the resonance critical value υ_a, at which the strongest hybridization takes place. Indeed, the other two spectral branches that change are

$$\bar{\beta}_{|-1,-1\rangle} \approx \tilde{\beta}_1 - 2\upsilon + 2\upsilon_a\xi^2, \quad \bar{\beta}_{|-1,1\rangle} \approx \tilde{\beta}_1 - 2\upsilon_a\xi^2. \tag{49}$$

Since the spectra for $l=0$ branches do not renormalize, one can obtain from Eqs. (45) and (49) the novel positions of the intersection points. The first point corresponds to intersection of $\bar{\beta}_{|1,-1\rangle}$ and $\bar{\beta}_{|1,0\rangle}$ curves

$$\upsilon_{a1} = \upsilon_a - 2\upsilon_a\xi^2, \tag{50}$$

whereas the curves $\bar{\beta}_{|-1,-1\rangle}$ and $\bar{\beta}_{|-1,0\rangle}$ intersect in the point

$$\upsilon_{a2} = \upsilon_a + 2\upsilon_a\xi^2. \tag{51}$$

This splitting is schematically shown in Fig. 7.

It should be emphasized that this effect is rather small in comparison with form birefringence in straight elliptical fibers

$$\upsilon_{a2} - \upsilon_{a1} = 2\frac{D}{4\upsilon_a\tilde{\beta}}\frac{D}{2\tilde{\beta}}. \tag{52}$$

Here the factor $D/2\tilde{\beta}$ is the form birefringence (difference in propagation constants of LP_{11} modes with opposite oddity) in a straight elliptical fiber. The factor $D/4\upsilon_a\tilde{\beta}$ conveys the so-called twisting-induced suppression of PMD. Using the definition of υ_a, one readily obtains for relative splitting

$$\frac{\upsilon_{a2} - \upsilon_{a1}}{\upsilon_a} = \frac{D^2}{4(\tilde{\beta}_1 - \tilde{\beta}_0)^2\tilde{\beta}^2}. \tag{53}$$

For example, for the fiber with strong ellipticity, mentioned in Ref. [35], with major and minor axes 6 and 3 μm, respectively, one obtains a significant splitting. Rough estimates give $\Delta\upsilon_a/\upsilon_a \approx 0.2$ (at $\delta=0.33$). However, for HCFs with small ellipticity the splitting rapidly decreases: at $\delta=0.05$ one has $\Delta\upsilon_a/\upsilon_a = 2.9\times10^{-3}$. The phenomenon of PMD reduction is well known in fiber optics both for the fundamental and higher-order modes [49]. If one does not allow for that effect, one may arrive at a wrong conclusion on a linear in D splitting of the resonance points. In particular, this mistake was made in Ref. [31], where the expressions for form birefringence of straight fibers [41] had been applied for twisted geometry.

VI. CONCLUSION

In the present paper we have theoretically studied generation and conversion of OVs in long-period helical core fibers produced by drawing from a perform with an eccentric core. We have shown that this type of HCF possesses analogous properties to the HCFs produced by periodic bending. We have shown that in such fibers topologically induced phase corrections lead to convergence of spectral curves, and at the intersection points a resonant coupling between the fundamental and the vortex modes occurs, as well as coupling between OVs, whose topological charges differ by unity. This coupling leads to energy exchange between the coupled modes, which brings forth various conversion phenomena (e.g., fundamental mode-OV, OV-OV) and the like. We have studied transmittance spectra for conversion of the fundamental mode into an OV and shown that this effect can be used for creation of all-fiber generator of OVs from GBs. We have also demonstrated that such fibers can be used for rising or lowering the topological charge of the input OV by unity. In addition, we have studied effect of elliptic deformation of the preform's core on transformation properties of HCFs and shown that this leads to splitting of resonance torsions (or wavelengths) for conversion of left and right circularly polarized input beams. We have emphasized that one can neglect this effect in long-period HCFs because of PMD reduction in twisted fibers.

[1] M. Vasnetsov and K. Staliunas, *Optical Vortices* (Nova Science, Huntington, NY, 1999), Vol. 228; A. Desyatnikov, Yu. Kivshar, and L. Torner, Prog. Opt. **47**, 291 (2005).
[2] M. S. Soskin and M. V. Vasnetsov, Prog. Opt. **42**, 219 (2001).
[3] G. A. Swartzlander, Jr., "Singular Optics/Optical Vortex References," http://www.u.arizona.edu/~grovers/SO/so.html
[4] J. F. Nye and M. V. Berry, Proc. R. Soc. London, Ser. A **336**, 165 (1974).
[5] L. Allen, M. J. Padgett, and M. Babiker, Prog. Opt. **39**, 291 (1999); S. Franke-Arnold, L. Allen, and M. Padgett, Laser Photonics Rev. **2**, 299 (2008).
[6] L. Allen, S. M. Barnett, and M. J. Padgett, *Optical Angular Momentum* (IOP Publishing, Bristol, 2003).
[7] G. S. Agarwal and J. Banerji, Opt. Lett. **27**, 800 (2002).
[8] G. Gibson, J. Courtial, M. J. Padgett, M. Vasnetsov, V. Pas'ko, S. M. Barnett, and S. Franke-Arnold, Opt. Express **12**, 5448 (2004).
[9] Z. Bouchal and R. Chelechovsky, New J. Phys. **6**, 131 (2004).
[10] J. A. Anguita, M. A. Neifeld, and B. V. Vasic, Appl. Opt. **47**, 2414 (2008).
[11] T. Gahagan and G. A. Swartzlander, Jr., Opt. Lett. **21**, 827 (1996); W. M. Lee, B. P. S. Ahluwalia, X.-C. Yuan, W. C. Cheong, and K. Dholakia, J. Opt. A, Pure Appl. Opt. **7**, 1 (2005); V. Garces-Chavez, K. Volke-Sepulveda, S. Chavez-Cerda, W. Sibbett, and K. Dholakia, Phys. Rev. A **66**, 063402 (2002); H. He, M. E. J. Friese, N. R. Heckenberg, and H. Rubinsztein-Dunlop, Phys. Rev. Lett. **75**, 826 (1995).
[12] G. H. Lee, G. Foo, E. G. Johnson, and G. A. Shwartzlander, Jr., Phys. Rev. Lett. **97**, 053901 (2006); F. Tamburini, G. Anzolin, G. Umbriaco, A. Bianchini, and C. Barbieri, *ibid.* **97**, 163903 (2006); G. A. Shwartzlander, Jr., E. L. Ford, R. S. Abdul-Malik, L. M. Close, M. A. Peters, D. M. Palacios, and D. W. Wilson, Opt. Express **16**, 10200 (2008).
[13] B. Spektor, A. Normatov, and J. Shamir, Appl. Opt. **47**, A78 (2008).
[14] A. G. Peele and K. A. Nugent, Opt. Express **11**, 2315 (2003).
[15] S. Thanvanthri, K. T. Kapale, and J. P. Dowling, Phys. Rev. A **77**, 053825 (2008).
[16] P. S. Tan, X.-C. Yuan, J. Lin, Q. Wang, T. Mei, R. E. Burge, and G. G. Mu, Appl. Phys. Lett. **92**, 111108 (2008).
[17] K. O'Holleran, M. R. Dennis, F. Flossmann, and M. J. Padgett, Phys. Rev. Lett. **100**, 053902 (2008).
[18] J. F. Nye, *Natural Focusing and Fine Structure of Light: Caustics and Wave Dislocation* (IOP Publishing, Bristol, 1999); M. V. Berry, J. Opt. A, Pure Appl. Opt. **6**, 475 (2004); I. Freund, M. S. Soskin, and A. I. Mokhun, Opt. Commun. **208**, 223 (2002); F. Flossmann, K. O'Holleran, M. R. Dennis, and M. J. Padgett, Phys. Rev. Lett. **100**, 203902 (2008).
[19] I. I. Mokhun, in *Optical Correlation Techniques and Applications* (SPIE Press, Bellingham, 2007) p. 1; I. Mokhun and R. Khrobatin, J. Opt. A, Pure Appl. Opt. **10**, 064015 (2008).
[20] A. Ya. Bekshaev and M. S. Soskin, Opt. Commun. **271**, 332 (2007).
[21] M. W. Beijersbergen, L. Allen, H. E. L. O. van der Ween, and J. P. Woerdman, Opt. Commun. **96**, 123 (1993); J. Courtial and M. J. Padgett, *ibid.* **159**, 13 (1999); E. Abramochkin and V. Volostnikov, *ibid.* **83**, 123 (1991).
[22] M. W. Beijersbergen, R. P. C. Coerwinkel, M. Kristensen, and J. P. Woerdman, Opt. Commun. **112**, 321 (1994); X.-C. Yuan, J. Lin, J. Bu, and R. E. Burge, Opt. Express **16**, 13599 (2008).
[23] N. R. Heckenberg, R. McDuff, C. P. Smith, and A. G. White, Opt. Lett. **17**, 221 (1992); V. Yu. Bazhenov, M. S. Soskin, and M. V. Vasnetsov, J. Mod. Opt. **39**, 985 (1992).
[24] Y. J. Liu, X. W. Sun, D. Luo, and Z. Raszewsk, Appl. Phys. Lett. **92**, 101114 (2008).
[25] Ya. V. Izdebskaya, V. G. Shvedov, and A. V. Volyar, Opt. Lett. **30**, 2472 (2005); V. G. Shvedov, Ya. V. Izdebskaya, A. N. Alekseev, and A. V. Volyar, Tech. Phys. Lett. **28**, 256 (2002).
[26] K. J. Webb and M.-C. Yang, Phys. Rev. E **74**, 016601 (2006).
[27] Z. Bouchal, O. Haderka, and R. Chelechovsky, New J. Phys. **7**, 125 (2005).
[28] D. McGloin, N. B. Simpson, and M. J. Padgett, Appl. Opt. **37**, 469 (1998).
[29] E. G. Johnson, J. Stack, and C. Kochler, J. Lightwave Technol. **19**, 753 (2001).
[30] C. N. Alexeyev, A. V. Volyar, and M. A. Yavorsky, J. Opt. A, Pure Appl. Opt. **8**, L5 (2006).
[31] C. D. Poole, C. D. Townsend, and K. T. Nelson, J. Lightwave Technol. **9**, 598 (1991).
[32] H. F. Taylor, J. Lightwave Technol. LT- **2**, 617 (1984); J. N. Blake, B. Y. Kim, and H. J. Shaw, Opt. Lett. **11**, 177 (1986).
[33] K. S. Lee, Opt. Commun. **198**, 317 (2001); K. S. Lee and T. Erdogan, Electron. Lett. **37**, 156 (2001); K. S. Lee and T. Erdogan, J. Opt. Soc. Am. A **18**, 1176 (2001).
[34] V. I. Kopp and A. Z. Genack, Opt. Lett. **28**, 1876 (2003); V. I. Kopp, V. M. Churikov, J. Singer, N. Chao, D. Neugroschl, and A. Z. Genack, Science **305**, 74 (2004); V. I. Kopp, V. M. Churikov, and A. Z. Genack, Opt. Lett. **31**, 571 (2006); V. I. Kopp, A. Z. Genack, V. M. Churikov, J. Singer, and N. Chao, Photonics Spectra **38**, 78 (2004).
[35] V. I. Kopp, V. M. Churikov, G. Zhang, J. Singer, C. W. Draper, N. Chao, D. Neugroschl, and A. Z. Genack, J. Opt. Soc. Am. B **24**, A48 (2007).
[36] C. N. Alexeyev, B. P. Lapin, and M. A. Yavorsky, Phys. Rev. A **78**, 013813 (2008).
[37] S. Oh, K. R. Lee, U.-C. Paek, and Y. Chung, Opt. Lett. **29**, 1464 (2004).
[38] W. Shin, B.-A. Yu, Y.-C. Noh, J. Lee, D.-K. Ko, and K. Oh, Opt. Lett. **32**, 1214 (2007).
[39] Z. Jiang and J. R. Marciante, J. Opt. Soc. Am. B **23**, 2051 (2006).
[40] Z. Menachem and M. Mond, PIER **61**, 159 (2006).
[41] A. W. Snyder, J. D. Love, *Optical Waveguide Theory* (Chapman and Hall, London, 1985).
[42] G. A. Korn and T. M. Korn, *Mathematical Handbook for Scientists and Engineers* (McGraw Hill, New York, 1968).
[43] C. N. Alexeyev, B. A. Lapin, and M. A. Yavorsky, J. Opt. Soc. Am. B **24**, 2666 (2007).
[44] C. N. Alexeyev, A. V. Volyar, and M. A. Yavorsky, in *Lasers, Optics and Electro-Optics Research Trends*, edited by Lian I. Chen (Nova Publishers, New York, 2007), p. 131.
[45] A. S. Davydov, *Quantum Mechanics* (Pergamon, Oxford, 1976).
[46] C. N. Alexeyev, B. P. Lapin, and M. A. Yavorsky, Ukr. J. Phys. Opt. **9**, 34 (2008).

[47] C. N. Alexeyev and M. A. Yavorsky, J. Opt. A, Pure Appl. Opt. **9**, 6 (2007); K. Yu. Bliokh, Phys. Rev. Lett. **97**, 043901 (2006).

[48] C. N. Alexeyev and M. A. Yavorsky, J. Opt. A, Pure Appl. Opt. **6**, 824 (2004).

[49] M. Wang, T. Li, and S. Jian, Opt. Express **11**, 2403 (2003); A. Galtarossa and C. R. Menyuk, *Polarization Mode Dispersion. Optical and Fiber Communications Reports* (Springer-Verlag, New-York, 2005).